Vision Research 154 (2019) 115–121

Contents lists available at ScienceDirect

Vision Research

journal homepage: www.elsevier.com/locate/visres

Comprehensive optical design model of the goldfish eye and quantitative simulation of the consequences on the accommodation mechanism

Ilka Claus[a,*], Katharina Frey[a,1], Tobias Hönle[a,b,1], Robert Brüning[a,b,1], Andreas Reichenbach[c,2], Mike Francke[c,d,2], Robert Brunner[a,b,1]

[a] Ernst-Abbe-Hochschule, University of Applied Sciences Jena, Germany
[b] Fraunhofer Institute of Applied Optics and Precision Engineering (IOF), Jena, Germany
[c] Paul-Flechsig-Institute for Brain Research, Department of Pathophysiology of Neuroglia, University Leipzig, Germany
[d] Saxonian Incubator of Clinical Translation (SIKT), University Leipzig, Germany

ARTICLE INFO

No. of reviewers: 1

Keywords:
Goldfish eye model
Gradient index lens
Accommodation
Depth of field

ABSTRACT

To further extent our understanding of aquatic vision, we introduce a complete optical model of a goldfish eye, which comprises all important optical parameters for the first time. Especially a spherical gradient index structure for the crystalline lens was included, thus allowing a detailed analysis of image quality, regarding spot size, and wavelength dependent aberration. The simulation results show, that our realistic eye model generates a sufficient image quality, with a spot radius of 4.9 µm which is below the inter cone distance of 5.5 µm. Furthermore, we optically simulate potential mechanical processes of accommodation and compare the results with contradictory findings of previous experimental studies. The quantitative simulation of the accommodation capacity shows that the depth of field is strongly dependent on the resting position and becomes significantly smaller when shorter resting positions are assumed. That means, to enable an extended depth perception with high acuity for the goldfish an adaptive, lens shifting mechanism would be required. In addition, our model allows a clear prediction of the expected axial lens-shift, which is necessary to ensure a sufficient resolution over a large object range.

1. Introduction

Aquatic vertebrates have a rigid, spherical lens to compensate the refractive loss of the cornea in underwater conditions. Therefore, they need to implement other accommodation strategies than terrestrial animals. This mechanism has been qualitatively investigated for teleost fish. One of the first studies was conducted by Beer (1894). He investigated the accommodation mechanism of many different teleost species by retinoscopy after electrical stimulation or administration of medication. He found that most teleosts have a slightly myopic refractive state. His investigations have also shown that the accommodation is not caused by a change of the lens curvature, as in many terrestrial vertebrates, but by a lens shift. Beer was able to prove negative accommodation in the majority of teleost species that he studied. This means that the unaccommodated eye focuses on near objects. In order to resolve distance object, the optical system is actively adapted by moving the lens toward the retina.

His results were later confirmed by several experimental studies (Fernald, 1991; Kimura & Tamura, 1966; Sivak, 1973; Walls, 1963).

One of the investigated teleost species was the goldfish, for which different experimental studies on their accommodation capabilities show inconsistent conclusions. For example, Somiya and Tamura (1973) investigated the lens shift of the enucleated eye of the goldfish on the basis of photographs before and after electrical stimulation. They noticed a slight lens movement toward the retina. However, the exact distance could not be determined and a nasal-temporal displacement could not be observed. Also, Sivak (1973) observed an accommodation by means of retinoscopy and additional photographic control measurements after administration of atropine and pilocarpine. In contrast, the study of Kimura and Tamura (1966) found no lens shift by means of

* Corresponding author at: Ernst-Abbe-Hochschule Jena University of Applied Sciences, Carl-Zeiss-Promenade 2, 07745 Jena, Germany.
E-mail addresses: Ilka.Claus@eah-jena.de (I. Claus), Katharina.Frey@eah-jena.de (K. Frey), Tobias.Hoenle@eah-jena.de (T. Hönle), Robert.Bruening@eah-jena.de (R. Brüning), reia@medizin.uni-leipzig.de (A. Reichenbach), Mike.Francke@medizin.uni-leipzig.de (M. Francke), Robert.Brunner@eah-jena.de (R. Brunner).
[1] Ernst-Abbe-Hochschule Jena University of Applied Sciences, Carl-Zeiss-Promenade 2, 07745 Jena, Germany.
[2] Paul-Flechsig-Institute for Brain Research, Department of Pathophysiology of Neuroglia, University Leipzig, Liebigstr. 19, 04103 Leipzig, Germany.

https://doi.org/10.1016/j.visres.2018.11.005
Received 23 July 2018; Received in revised form 29 October 2018; Accepted 15 November 2018
Available online 29 November 2018

photographs after electrical stimulation of enucleated eyes. Also, Charman and Tucker (1973) could not confirm any accommodation mechanism by means of slit lamp examination and retinoscopy. They assumed that the eye's depth of field is sufficient and, thus, no accommodative movement of the lens is necessary. In addition, Frech (2009) and Frech, Vogtsberger, and Neumeyer (2012) investigated the refractive state of a single goldfish using infrared photoretinoscopy in a training experiment. They presented objects at various distances from 10 to 40 cm and could not detect any variation in refractive power. Furthermore, contradictory to Beer's assumption that teleosts are myopic in the unaccommodated state, the experiment suggested that the goldfish eye may be hyperopic in a relaxed state of accommodation.

From the evaluation of the aforementioned studies, there is no clear evidence as to whether the goldfish eye accommodates or has a sufficient depth of field. The various results may be due to the use of very diverse experimental methods which, for the most part, do not reflect the natural behavior of goldfish. For most experiments, the lens movement was artificially induced by electrical stimulation or medication and was performed on an enucleated eye. Additionally, Fernald (1991) and Frech et al. (2012) themselves express uncertainty about the applicability of retinoscopy to investigate the refractive power of the goldfish eye because the precise source of the retinal reflection is not known. Should the reflecting layer and the focal plane not coincide, this would lead to a systematic absolute error. Some studies have shown that the goldfish is physiologically able to move the lens, but it is not clear, whether it uses this ability for accommodation (Somiya & Tamura, 1973; Sivak, 1973).

Currently, no quantitative investigations of the accommodation behavior based on optical simulation have been done, which results in an incomplete theoretical understanding of the vision of the goldfish eye, like the necessity of accommodation. To overcome this lack of investigation, we designed a realistic eye model that considered the geometric optic parameters, the refractive gradient index (GRIN) of the lens, the retinal specification, and the resting position. The individual components are widely known. A simplified model was already established by Charman and Tucker (1973) based on experimental measurement data. Their schematic model is emmetropic; it assumes the cornea as a single surface and contains a homogeneous lens with an index of 1.69. There are also studies on the GRIN profile of the lens (Axelrod, Lerner, & Sands, 1988; Jagger, 1992) and on the structure of the retina (Marc & Sperling, 1976; Neumeyer, 2003). To the best of our knowledge, an optical model which combines all components and thus enables a quantitative investigation of the optical quality and the consequence on accommodation mechanism, does not exist.

2. Methods

This chapter describes our strategy to develop a comprehensive model of the goldfish eye. The databases of the initial parameters and the optimization procedure are discussed. The framework of investigating the resulting image quality and the consequences on the accommodation mechanism are presented in detail.

2.1. Developing an optical goldfish eye model

To estimate the geometric optical parameters, the measurements of Charman and Tucker (1973) were used, enabling the development of an initial simulation model. Furthermore, our model takes into account that the goldfish in nature has a spherical gradient index lens, with a refractive index continuously and parabolically decreasing from the core to the cortex (Matthiessen, 1880). The GRIN distribution is based on the improved Matthiessen polynomial of Jagger (1992). For the cortical refractive index (n_{ctx}), a range between 1.37 and 1.38, and for the core (n_{core}), between 1.51 and 1.52, was used as a starting point (Jagger, 1992; Matthiessen, 1882).

In order to evaluate the resolution capability of the goldfish eye, studies about the retina properties were considered. According to the summary of Palacios, Varelab, Srivastavaa, and Goldsmith (1998), the goldfish retina contains four cone types with a corresponding spectral sensitivity of about 625 nm (L-cone), 535 nm (M-cone), 455 nm (S-cone), and 350 nm (UV-cone). The relative number of the L-, M- and S-cones are 0.45, 0.35, and 0.20, and UV-cones are rare (Marc & Sperling, 1976). Regarding visual acuity, the L-, M- and S-cone types have approximately the same contribution (Neumeyer, 2003). The contribution of the UV-cones is unknown and due to their small number, they will be not considered for the resolution criterion. The simulation was started with the medium wavelength of 535 nm.

Additionally, we assume that the resolution of the goldfish eye is limited by the average cone density (Neumeyer, 2003). The mean inter cone distance is approximately 11 µm corresponding to a resolution of 13.5' (Marc & Sperling, 1976; Neumeyer, 2003).

To complete our initial eye model, further details to the cornea, pupil, and the resting position are required. For these components, no specific values are available for the goldfish eye. Therefore, values of other fish and vertebrates were consulted and various assumptions were made.

First, we assumed that the front and the back surfaces of the cornea have nearly the same radius of curvature (Beer, 1894; Hughes, 1977) and the refractive index of the cornea is 1.376, as in various other vertebrates (Hughes, 1977).

Furthermore, we expect that the pupil is located approximately halfway between lens anterior vertex and equator, adapted from research on the rainbow trout (Jagger & Sands, 1996).

In conclusion, based on Beer's research (1984), we assumed that the goldfish has a negative accommodation mechanism and thus its eye focus on near objects at the resting position. Beer's research is consistent with Fernald (1991) indicating the poor underwater visibility caused by scattering and turbidity and stating the unlikeliness of the teleosts ability to see clearly in the distance at the unaccommodated state.

The exact visual range of the goldfish is still not known. Experimental results carried out by Neumeyer (2003) targeting the visual acuity in goldfish uses an object distance of 30 mm. Therefore, one can assume that goldfish can see clearly at this distance. Thus, we used this visual distance as the smallest possible resting position. Consequently, the resting position can be seen as the object distance for which the goldfish focuses without accommodation and will be used for adjusting the eye model.

A schematic representation of the goldfish eye is shown in Fig. 1. The illustration contains all relevant optical components: the cornea; the anterior chamber with the aqueous humor; the iris as aperture; the spherical lens, which is responsible for the main refractive power to focus light onto the retina; the vitreous body as stabilizer; and the retina with the receptor cells as imaging layer.

To simulate and optimize our eye model, we used the raytracing software Optic Studio, which allows the performance evaluation of the eye model by a geometric optical approach. For the simulations, the initial eye model was optimized regarding the constraint values based on the geometrical data basis and the GRIN distribution of the improved Matthiessen polynomial with the objective of achieving a sufficient

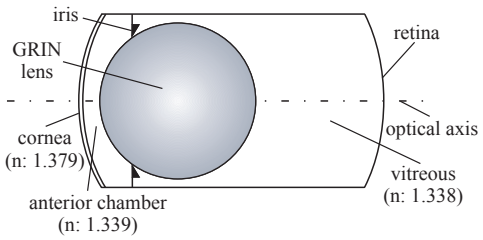

Fig. 1. Schematic representation of the vertical section of a goldfish eye.

resolution. The resolution capability was evaluated by investigating the spot diagrams. The root-mean-square radius (RMS radius) of the spot must be smaller than the permissible cone radius of 5.5 µm. All simulations were initially performed for the mean wavelength of 535 nm, a pupil diameter of 1.8 mm, and for object distance of 30 mm.

To simulate the spherical GRIN lens, a polynomial expansion for the varying refractive index distribution was used (Oslo, 2016):

$$n = n_{ctx} + A(r - R) + B(r - R)^2 + C(r - R)^3 + D(r - R)^4 \quad (1)$$

with

$$r = \frac{R}{|R|}\sqrt{x^2 + y^2 + (R - z)^2} \quad (2)$$

The formula describes the index profile of the three-dimensional spherical lens model consisting of spherical shells arranged around the center of the lens. The coordinate system origin is located at the front lens vertex. R is the radius of curvature of the spherical lens in mm measured at the vertex; r is composed of the radial coordinates x, y, and z within the lens; n_{ctx} is the refractive index at the cortex; and A, B, C, and D are coefficients for adjusting the refractive index profile. (OpticStudio, 2016).

Due to the lack of a common definition about the focus distance in the unaccommodated state, our eye model was optimized for different near-point positions. When changing the resting position, the initial model must be adapted. For this, the lens radius of curvature, the depth of the vitreous body, the anterior chamber depth, the focal length, and the GRIN coefficients are variably set within the given limits and further optimization occurs. The different eye models are denoted in the following with Model_Rx, where x stands for the distance of the respective unaccommodated position in mm (e.g., Model_R30 for a resting position of 30 mm).

2.2. Simulation and investigation of the consequence on accommodation mechanism

To get a first impression on the image quality dependency from the object distance, the RMS radius change of each eye model was evaluated with respect to the object distance enlargement while the eye model remained unchanged. Subsequently, the depth of field was determinable for each model as the anterior and posterior range (δ_{ant} and δ_{post}) in which the spot size remains below the resolution criteria of 5.5 µm ($1/2\ z' \approx$ cone radius). This is illustrated in Fig. 2. Starting from the resting position (a_0), the object (y) was moved forwards (a_{ant}) or backwards (a_{post}) until the resolution limit (z') was reached.

Beyond this range, it is assumed that an object can no longer be resolved. Hence, to extend the visual range, an accommodation mechanism, like refocus by shifting the lens along the optical axis towards the retina, would be required. In that case, the necessary amount of lens movement was determined by optimizing only the anterior chamber depth and adjusting the vitreous body length so that the total length remains unchanged.

To investigate whether other wavelengths have an influence on the depth of field, the eye model was also adjusted for 455 nm (S-cone) and 625 nm (L-cone). Since our GRIN lens neglects all dispersion effects, the refractive index was adjusted with respect to the used wavelength. For that purpose, the experimentally observed chromatic focal length differences of approximately 5% for the goldfish were used (Kreuzer & Sivak, 1985; Sivak & Bobier, 1978). Since no data for the dispersion and Abbe numbers are available for the goldfish eye, we used the research results from Jagger (1992) for our simulations. He assumed an Abbe number for the fish lens of 50 and 38 for the cortex (n_{ctx}: 1.38) and the core (n_{core}: 1.52), respectively, on the basis of the focal length differences of the rainbow trout and the dispersion data of a cat's eye.

3. Results

This section presents the resulting eye model with the obtained parameters, the simulation results for image quality, and the consequence on accommodation behavior.

3.1. Optical eye model

The previously discussed geometrical and optical constraints and assumptions result in a comprehensive goldfish eye model. The parameters for the adjusted model for a wavelength of 535 nm, an aperture diameter of 1.8 mm (Charman & Tucker, 1973; Jagger, 1992), and an exemplary resting position of 30 mm are shown in Table 1.

Furthermore, the pupil is located 0.419 mm behind the lens anterior surface (d_p). The comprehensive eye model has a total length of 4.289 mm and a focal length (FL) of 2.748 mm. The Matthiessen ratio (distance from centre of lens to retina/ lens radius of curvature) (Shand, Døving, & Collin, 1999) is 2.55 times the radius (R). In order to model the index distribution of the GRIN lens, the improved Matthiessen polynomial approach from Jagger was approximated by the polynomial function given in Eq. 1. From the optimization, the best results were found for a cortex index of 1.369, a core index of 1.536 and the coefficients A: −0.3804, B: −0.3255, C: −0.1498, and D: −0.0385. The GRIN distribution corresponds well with the improved Matthiessen polynomial from Jagger (1992).

The comprehensive optimized Model_R30 is shown in Fig. 3A with the ray paths for the incident angles 0, 1, 3, and 5°. In addition, the major distances are shown: corneal thickness (d_1), anterior chamber depth (d_2), lens diameter (d_3), vitreous body depth (d_4), and pupil distance (d_p). To evaluate the achievable image quality, the spot diagrams shown in Fig. 3B were analyzed.

The spot diagrams show that the goldfish reaches a sufficiently good resolution. Even up to 3.3° incident angle the RMS radius is smaller than the permissible RMS radius of 5.5 µm (cone radius). On axis, the RMS radius is 4.83 µm, resulting in a theoretical resolution of 11.54', and thus providing a sufficient image quality.

As another example, the modified lens radius of curvature for Model_R50 is 1.175 mm, the anterior chamber depth is also 0.25 mm,

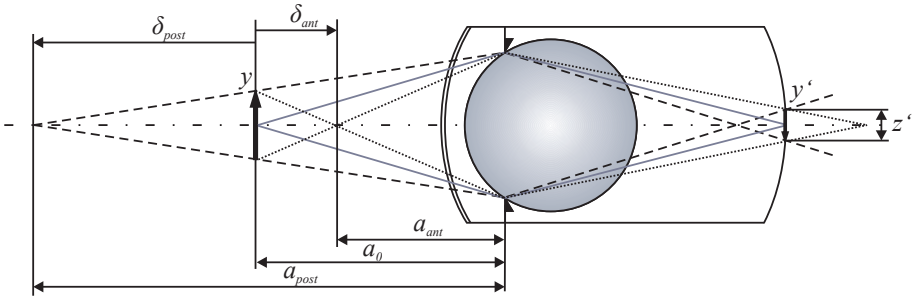

Fig. 2. Schematic ray diagram to illustrate the depth of field (anterior (δ_{ant}) and posterior (δ_{post}) range), adapted from Pedrotti et al. (2002), with: a_0: starting distance, a_{ant}: anterior distance, a_{post}: posterior distance.

Table 1
Parameters of the adjusted goldfish eye model.

Surface	Parameter	Radius of curvature [mm]	Distance [mm]	Refractive Index at 535 nm
0	Object	–	30.000	1.335
1	Cornea	2.500	0.038	1.379
2	Anterior Chamber	2.501	0.250	1.339
3	Lens	1.127	2.253	GRIN
4	Vitreous	− 1.127	1.748	1.338
5	Retina	− 2.860	–	–

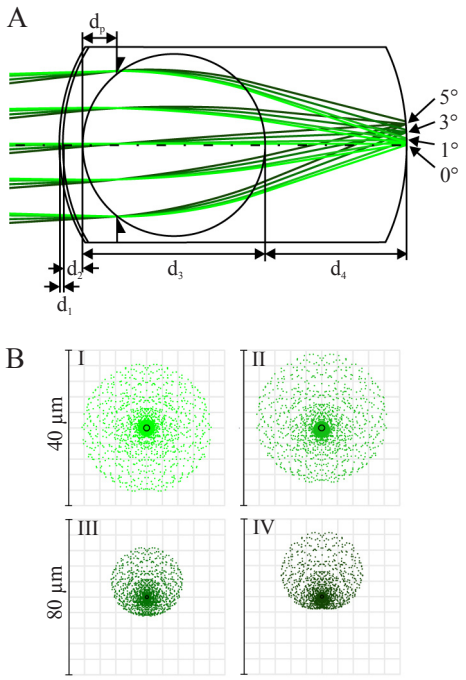

Fig. 3. (A) Optical design model of the goldfish eye for a resting position of 30 mm, with: d_1: corneal thickness, d_2: anterior chamber depth, d_3: lens diameter, d_4: vitreous body depth, d_p: pupil distance, (B) Corresponding spot diagrams for various incident angles: I: 0° (RMS radius 4.83 µm), II: 1° (RMS radius 4.89 µm), III: 3° (RMS radius 5.38 µm), IV: 5° (RMS radius 6.31 µm).

and the vitreous body depth is 1.746 mm. The total length is 4.38 mm. The focal length is 2.829 mm and the Matthiessen ratio is 2,49. The GRIN coefficients are A: −0.3753, B: −0.3375, C: −0.1747, D: −0.0477. The model achieves an RMS radius of 1.31 µm, resulting in a theoretical resolution of 3.09'. The resolution is for an incident angle over 10° smaller than the inter cone distance.

For the representative described Model_R30 and Model_R50, all geometric parameters are within the given measuring ranges of Charman and Tucker (1973).

The refractive index of the core (1.536) and the cortex (1.369) are close to the values of Jagger (1992) and Matthiessen (1882) and within the measurement range of Axelrod et al. (1988). The pupil is located 0.42 mm behind the lens vertex, which corresponds with the data of (Jagger & Sands, 1996) that the pupil of the rainbow trout lies halfway between lens anterior vertex and equator.

Additionally, the GRIN distribution of the lens is comparable with the parabolic profile of the improved Matthiessen polynomial by Jagger (1992). The Model_R30 achieves with 11.54' a lower resolution than Jagger's single lens in medium, which reached a resolution of 2'. However, the spot radius is well below the average cone radius. The lower resolution compared to Jagger may be due to his simplified approach of considering only a single lens in medium and not the entire eye. In addition the object distance of the two models differs considerably. Jagger's model is adapted for an infinity object distance and our model for an distance of 30 mm. For Model_R50 the resolution could be improved to 3.09'.

The optimization of the comprehensive eye model for other cases of resting positions resulted in slightly different values for geometrical parameters, as shown for Model_R50. All models provided also a sufficient image quality and are within the expected range of the literature values. In general, the results suggest that the models are suitable for further investigation.

3.2. Consequences on accommodation behavior

With the simulated eye model, we investigated how the image quality behaves for different object distances while the optical system remains unchanged. Fig. 4 shows the corresponding spot diagrams for the distances 30, 50, 100, and 400 mm for Model_R30 (A) and Model_R50 (B). Even small changes of the object distance result in a considerable increase of the RMS radius. For Model_R30, a small displacement from 30 to 50 mm leads to an RMS radius increase of 15.68 µm. As a consequence, the depth of field for Model_R30 only reaches from 29.4 to 33.6 mm. For Model_R50, a displacement from 50 to 100 mm leads to an increase of 15.92 mm. Increasing the focus distance for the resting position to 50 mm extends the depth of field slightly to a range of 43.4–59.8 mm. For both models, an accommodation by lens movement would be necessary to image distant objects within the resolution criteria.

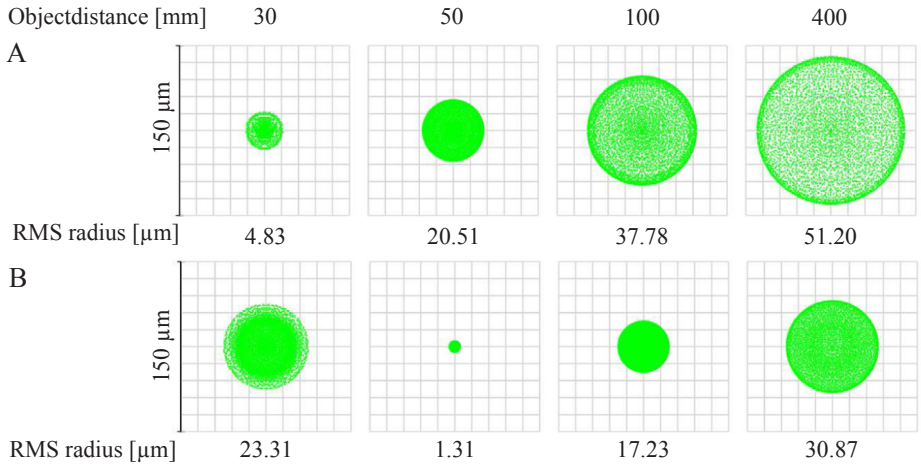

Fig. 4. Spot diagrams for (A) Model_R30 and (B) Model_R50, for different object distances (30, 50, 100 and 400 mm) without refocusing.

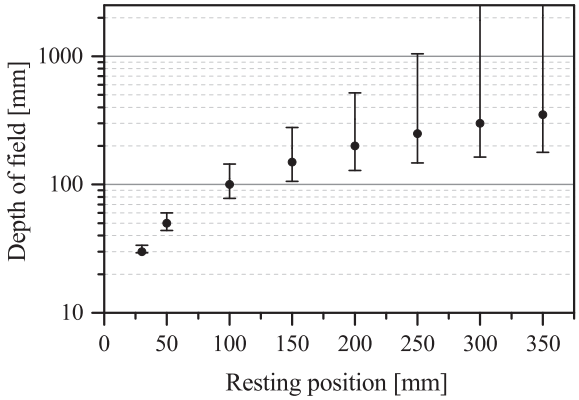

Fig. 5. Dependence of the depth of field on the resting position, for a permissible RMS radius of 5.5 µm, with: dots: resting position (a_0), vertical lines: corresponding depth of field range, horizontal lines: upper (a_{post}) and lower limit (a_{ant}) of the respective depths of field range.

Table 2
Depth of field for models with various resting positions.

a_0 [mm]	a_{ant} [mm]	a_{post} [mm]
30	29.4	33.6
50	43.9	60.0
100	78.2	144.6
150	105.8	278.9
200	128.5	518.6
250	147.5	1043.0
300	163.4	3643.0
350	178.0	> 10000

Since it has not yet been clarified which resting position goldfish possess and what influence it has on the depth of field, further models with different resting positions (100, 150, 200, 250, 300, and 350 mm) were investigated to evaluate the necessity of an accommodation mechanism. The results are shown in Fig. 5 and Table 2. The dots in Fig. 5 represent the respective resting position (a_0), the vertical lines represent the corresponding depth of field range, and the horizontal lines represent the upper (a_{post}) and lower limit (a_{ant}) of the respective depths of field range. It is notable that the depth of field depends on the resting position.

For small resting positions, the depth of field is very limited and an accommodation has to be made to resolve distant objects. An enlargement of the resting position results in an increasing depth of field range. From a resting position of 250 mm, a large object distance (147.5–1043 mm) can be imaged sufficiently on the retina. However, objects closer than 147.5 mm cannot be seen with the maximum resolution capability. Hence, should the goldfish be able to well resolve

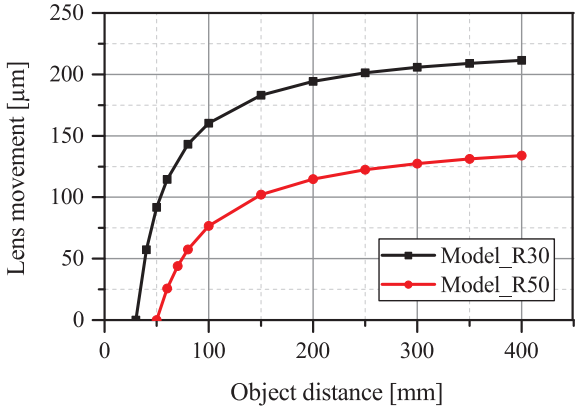

Fig. 7. Dependence of lens movement on object distance for Model_R30 and Model_R50.

Table 3
GRIN lens parameters and focal length for wavelength 455, 535, and 625 nm, Model_R30.

Wavelength [nm]	455	535	625
n_{ctx}	1.374	1.369	1.365
n_{core}	1.546	1.536	1.530
A	− 0.4285	− 0.3804	− 0.3487
B	− 0.4825	− 0.3255	− 0.2227
C	− 0.3291	− 0.1498	− 0.0324
D	− 0.1048	− 0.0385	0.0050
Focal length [mm]	2.650	2.748	2.799

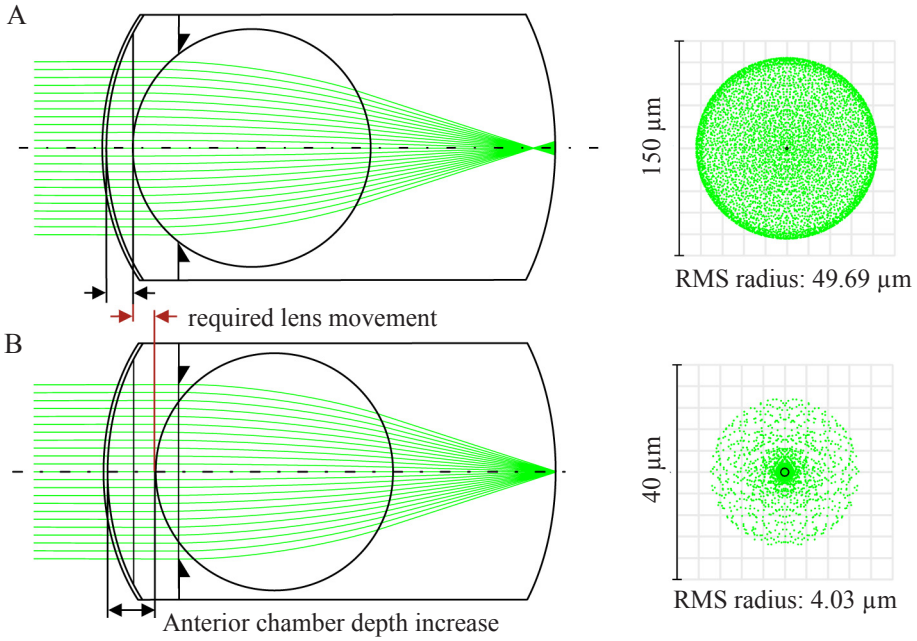

Fig. 6. (A) Model_R30 with an object in 300 mm distance, (B) required lens shift to see an object in 300 mm sharp.

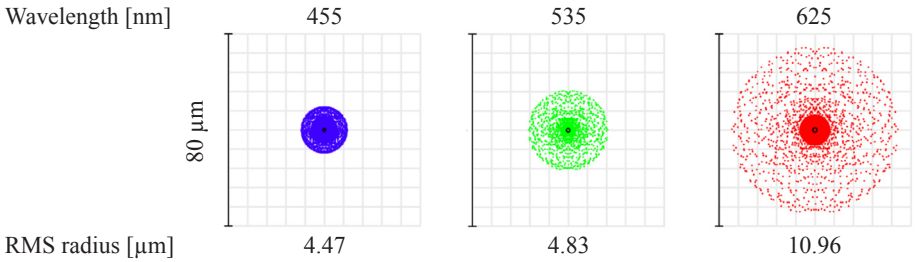

Fig. 8. Spot diagrams for Model_R30 for wavelength 455, 535, and 625 nm, object distance 30 mm.

closer objects, the eye must have a shorter resting position and a corresponding adjustment mechanism.

With increasing object distance, the image quality decreases, since the focus shifts towards the lens resulting in a blurry spot on the retina and an enlargement of the spot diameter. This is illustrated in the spot diagrams in Fig. 6A and the corresponding ray paths for the Model_R30. There an object point located at a distance of 300 mm imaged in front of the retina. By a lens shift, this focus drift could be compensated and the image would again be located at the retina, as depicted in Fig. 6B. Hence, in this case, the image quality for far distances could be clearly improved by accommodation.

Therefore, in the next step, we determined the necessary lens movement to accommodate and extend the imaging field range. The results for the Model_R30 and the Model_R50 are illustrated in Fig. 7. There, both curves steeply increase at the beginning and flatten for far object distances. In addition, it becomes clear that the amount of the lens shift depends on the resting position. For Model_R30, the necessary lens shift to image objects at a distance of 50 mm is already 92 µm. The total lens shift for resolving objects from 30 mm to over 350 mm is 209 µm. From the object distance of approximately 350 mm, the depth of field is sufficiently extended to see objects from over 10 m clearly, and no additional accommodation is required (see Fig. 5). For Model_R50, a lens movement of about 131 µm is sufficient.

According to the literature, lens movements from 150 µm could be measured for different teleosts (Somiya & Tamura, 1973). However, for the goldfish only a small shift was observed, without being able to measure the amount. Therefore, it is possible that the goldfish eye has a greater resting position than 30 mm. The further the resting position is, the smaller the necessary lens movement is (see Fig. 7). For example, it is possible that the lens shift of 131 µm which was determined for Model_R50 was outside the measuring range of Somiya and Tamura (1973).

In the last step, the influence of all three wavelengths on the depth of field was considered. The refractive indices and GRIN parameters resulting from the adjustment are presented in Table 3. Thus, a focal length difference of 5.4% and an Abbe number of approximately 50 for the cortex and 39 for the core could be achieved. The values correspond well with the assumptions made in the literature (Jagger, 1992; Kreuzer & Sivak, 1985; Sivak & Bobier, 1978).

As shown in Fig. 8 for the blue wavelength (455 nm) an RMS radius of 4.47 µm can be achieved which is in the range of the inter cone distance. The depth of field for the blue wavelength ranges from 27.0 to 31.0 mm. For the red wavelength the RMS radius (10.96 µm) is greater than the inter cone distance. The slightly poorer image quality for red results from the choice of the refractive indices. By using a lower index for the cortex and a higher index for the core a better image quality for green and thus a better image quality for red can be achieved. For our model we have tried to consider the specifications of Jagger (1992) and Matthiessen (1882) as well. For Model_R50 the image quality for red and blue is approximately the same. For all models, the consideration of all three wavelength does not lead to a significant enlargement of the depth of field.

4. Conclusion

Since it is difficult to investigate the accommodation behavior of the goldfish eye experimentally, in this work, a comprehensive eye model that allowed a quantitative analysis of the image quality and the consequence on accommodation was simulated. The simulated goldfish eye model includes all relevant specifications from previous experimental investigations: the optical geometrical parameters (Charman & Tucker, 1973), the gradient index distribution of the spherical lens (Jagger, 1992), the myopic resting position (Beer, 1894; Fernald, 1991), and the retina specifications (Marc & Sperling, 1976; Neumeyer, 2003). With the adjusted eye model, a sufficient image quality can be achieved, the resulting RMS radius of approximately 4.83 µm is below the cone radius of 5.5 µm. The good image quality and the correspondence of the individual parameters with the experimentally determined values from the literature justified the conclusion that the created goldfish eye model is suitable for further simulations.

The simulation results provided new knowledge regarding aquatic vision, especially accommodation behavior and depth of field. The investigations show, that without an adaptive mechanism the effective focus range of the goldfish eye is limited depending on the resting position. The smaller the resting position is, the lower is the depth of field range. This results in a very low depth of field range (29.4–33.6 mm) especially for the assumed short resting position of 30 mm. Should the depth of field of the eye be sufficient to focus objects in a large distance range, as assumed by Charman and Tucker (1973) according to our model a more distant resting position is probable. For example, with a resting position of 250 mm a depth of field ranging from 148 mm to more than 1 m can be well resolved. Since the goldfish in Neumeyer's (2003) training experiment achieved a visual resolution of approximately 15' (corresponds to a 6.2 µm spot radius) for an object distance of approximately 6 mm, it can be assumed that the near point of the goldfish is located close to the eye. In this case, the depth of field would be very limited and a lens shifting accommodation mechanism would be highly advantageous. Furthermore, the simulation results allow a clear quantitative prediction of the expected axial lens-shift, which is necessary to ensure a resolution smaller than the inter cone distance over an extended depth of field. The results of the determination of the depth of field and the potential lens shift can directly be used for the preparation of experimental verifications and validations.

Acknowledgments

I. Claus expresses thanks to the Ernst-Abbe-Hochschule Jena for the opportunity to take part in the PhD program of the University. This research was supported by a grant from the Deutsche Forschungsgemeinschaft to A.R. and M.F. (SPP1757; RE 849/16 and FR 1825/1–1).

References

Axelrod, D., Lerner, D., & Sands, P. J. (1988). Refractive index within the lens of a goldfish eye determined from the paths of thin laser beams. *Vision Research, 28*(1) 57–56.

Beer, T. (1894). Die Accommodation des Fischauges. *Archiv für die gesamte Pyhsiologie des Menschen und der Tiere, 58*(11–12), 523–650.
Charman, W. N., & Tucker, J. (1973). The optical system of the goldfish eye. *Vision Research, 13*(1), 1–8.
Fernald, R. D. (1991). Teleost vision: Seeing while growing. *Journal of Experimental Zoology, 256*(Suppl. 5), 167–180.
Frech, B. (2009). *Verhaltensphysiologische Analyse der visuellen Wahrnehmung räumlicher Tiefe beim Goldfisch.* Ph.D. thesisJohannes Gutenberg-Universitét Mainz.
Frech, B., Vogtsberger, M., & Neumeyer, C. (2012). Visual discrimination of objects differing in spatial depth by goldfish. *Journal of Comparative Physiology A, 198*(1), 53–60.
Hughes, A. (1977). *The Topography of Vision in Mammals of Contrasting Life Style: Comparative Optics and Retinal Organisation.* Berlin, Heidelberg: Springer, Berlin Heidelberg613–756.
Jagger, W. S. (1992). The optics of the spherical fish lens. *Vision Research, 32*(7), 1271–1284.
Jagger, W. S., & Sands, P. J. (1996). A wide-angle gradient index optical model of the crystalline lens and eye of the rainbow trout. *Vision Research, 36*(17), 2623–2639.
Kimura, K., & Tamura, T. (1966). On the direction of lens movement in visual accommodation of teleostean eyes. *Japanese Society of Scientific Fisheries, 32*(2), 112–116.
Kreuzer, R. O., & Sivak, J. G. (1985). Chromatic aberration of the vertebrate lens. *Ophthalmic & Physiological Optics, 5*(1), 33–41.
Marc, R. E., & Sperling, H. G. (1976). The chromatic organization of the goldfish cone mosaic. *Vision Research, 16*(11), 1211–1224.
Matthiessen, L. (1880). Untersuchungen über den Aplanatismus und die Periscopie der Krystalllinsen in den Augen der Fische. *Pflügers Archiv, 21*, 287–307.
Matthiessen, L. (1882). Über die Beziehung, welche zwischen dem Brechungsindex des Kerncentrums der Krystalllinse und den Dimensionen des Auges bestehen. *Pflügers Archiv, 27*, 510–523.
Neumeyer, C. (2003). Wavelength dependence of visual acuity in goldfish. *Journal of Comparativ Physiology A, 189*(11), 811–821.
OpticStudio. (2016). OpticStudio 16.5 SP1 Help files.
Oslo. (2016). Optics Software for Layout and Optimization - Program Reference 6.3.
Palacios, A. G., Varelab, F. J., Srivastavaa, R., & Goldsmith, T. H. (1998). Spectral sensitivity of cones in the goldfish, carassius auratus. *Vision Research, 38*(14), 2135–2146.
Pedrotti, F., Pedrotti, S., Bausch, W., & Schmidt, H. (2002). *Optik für Ingenieure – Grundlagen* (2. Auflage). Berlin, Heidelberg, New York: Springer-Verlag.
Shand, J., Døving, K. B., & Collin, S. P. (1999). Optics of the developing fish eye: comparisons of Matthiessen's ratio and the focal length of the lens in the black bream Acanthopagrus butcheri (Sparidae, Teleostei). *Vision Research, 39*(6), 1071–1078.
Sivak, J. G. (1973). Interrelation of feeding behavior and accommodative lens movements in some species of North American freshwater fishes. *Journal of the Fisheries Research Board of Canada, 30*(8), 1141–1146.
Sivak, J. G., & Bobier, W. R. (1978). Chromatic aberration of the fish eye and its effect on refractive state. *Vision Research, 18*(4), 453–455.
Somiya, H., & Tamura, T. (1973). Studies on the visual accommodation in fishes. *Japanese Journal of Ichthyology, 20*(4), 193–206.
Walls, G. L. (1963). *The vertebrate eye and its adaptive radiation.* New York, London: Hafner Publishing Company.